Wave Function of C_{70} in the Triplet State

X. L. R. Dauw, J. Visser, and E. J. J. Groenen*

Centre for the Study of Excited States of Molecules, Huygens Laboratory, Leiden University, P.O. Box 9504, 2300 RA Leiden, The Netherlands

Received: November 15, 2001; In Final Form: February 18, 2002

Results of a ^{13}C pulsed electron nuclear double resonance (ENDOR) study at 95 GHz of C_{70} in its photoexcited triplet state are reported. The C_{70} molecule of D_{5h} symmetry (an approximation for the triplet state) consists of 5 inequivalent types of carbon atoms, which we label 1 at the pole to 5 at the equator. The analysis of the ENDOR spectra reveals that the spin density is not uniformly distributed over the C_{70} molecule. About 66% of the spin density is on the atoms of type 3, 20% on the atoms of type 4, and 16% on the atoms of type 1, whereas no spin density is found on the atoms of type 2 and 5. The spin-density distribution in the triplet state for C_{70} is compared with that observed for C_{60} previously.

Introduction

Upon optical excitation of C_{60} or C_{70}, most molecules end up in the lowest triplet state, which for both fullerenes lies about 1.55 eV above the ground state[1,2] Besides this similarity, the triplet states have considerably different properties. Whereas the triplet state of C_{60} has a lifetime of about 400 μs,[3,4] the triplet state of C_{70} lives for about 50 ms,[3,5,6] and the phosphorescence yield is much larger for the latter.[4,7] For the C_{60} molecule the fine-structure parameter D is negative (−340 MHz),[3,8] whereas for C_{70} it is positive (+150 MHz).[3,6] To try and understand these differences, a detailed knowledge of the triplet wave function is required.

Recently, a W-band electron nuclear double resonance study has revealed the electron-spin-density distribution in the triplet state of C_{60}.[8] For C_{70}, such a detailed characterization of the triplet wave function is missing as yet. Until now, experimental studies involved electron paramagnetic resonance (EPR) and phosphorescence spectroscopy. For example, an electron spin−echo (ESE) study showed D to be positive and provided insight into the population and decay of the triplet sublevels.[6] Besides, the C_{70} molecule was found to pseudorotate around the fine-structure z-axis (long axis) at a rate of about once per microsecond at liquid-helium temperatures. The phosphorescence spectra of C_{70} in the Shpol'skii matrix n-pentane were found to be consistent with a triplet state of A_2' character.[7] (The label refers to D_{5h} symmetry, which concerns an approximation for C_{70} in the triplet state as follows from the nonzero value of the fine-structure parameter E[3]). Calculations on the triplet state of C_{70} have been performed by Surján et al., who reported a spin-density distribution for the lowest triplet state of A_2' character.[9] Most of the spin density was predicted to be on atoms of type 4, less on atoms of type 3, and a negative sign of D was calculated.

Here we present a pulsed ENDOR study at 95 GHz of a frozen solution of 15% ^{13}C enriched C_{70} at 1.5 K. Under D_{5h} symmetry, the C_{70} molecule comprises 5 types of symmetry inequivalent atoms.[10] We label these 1 to 5 (with abundances 10, 10, 20, 20, and 10, respectively), from the poles to the equator. On the basis of an orbital model, we analyze the ^{13}C hyperfine interaction derived from the ENDOR spectra in terms of a spin-density distribution in the triplet state. Each of the atoms of type 3 is found to carry about 3.3% of the total spin density. Smaller spin densities are found on the atoms of type 1 and 4, while the atoms of type 2 and 5 do not carry significant spin density. The experimental spin densities are compared to quantum-chemically calculated spin densities using a MINDO Hamiltonian. Finally, the wave function of the triplet state of C_{70} is compared with that for C_{60}.

Methods

A solution of 15% ^{13}C enriched C_{70} (MER) in decalin/cyclohexane (3:1 v/v) was studied at superfluid helium temperature (1.5 K). Pulsed EPR and ENDOR measurements were performed at W-band frequency on a home-built spectrometer[11] using a three-pulse microwave sequence ($p_1-\tau-p_2-T-p_3$). The length of the microwave pulses was 60 ns, T was 200 ms, and values for τ of 220 and 330 ns were used. For the ENDOR experiments, a radio frequency (RF) field was applied to the sample during the time T. Separate measurements were performed above and below 36 MHz and the RF coupling was adjusted manually for each experiment. Consequently, the relative intensity of both parts is known only approximately. In addition, a small variation of the RF coupling with frequency may have distorted the band shapes slightly. The triplet state was populated by continuous irradiation at 514 nm using a Spectra Physics 2017 Ar^+ laser.

Results

A W-band ESE-detected EPR spectrum of a frozen solution of C_{70} in decalin/cyclohexane at 1.5K is presented in Figure 1. It has been measured under continuous laser irradiation and therefore differs from the spectrum in ref 6 that was obtained upon pulsed laser excitation. The unconventional shape of this triplet EPR spectrum derives from $\Delta M_S = 2$ relaxation, which results from the pseudorotation of C_{70} in the triplet state.[6] The fields B_1 and B_2 at which the ENDOR experiments have been performed are indicated. For the fields B_1 and B_2 the signals derive from molecules that have their fine-structure z-axis closely parallel and perpendicular to the magnetic field, respectively.

* Corresponding author. Phone: +31-71-5275914. Fax: +31-71-5275819. E-mail: mat@molphys.leidenuniv.nl.

10.1021/jp014239t CCC: $22.00
Published on Web 03/21/2002

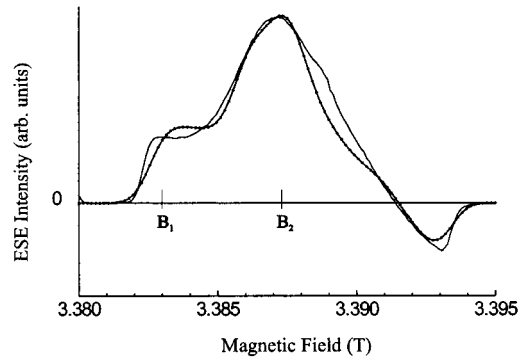

Figure 1. W-band ESE-detected EPR spectrum of C_{70} in decalin/cyclohexane at 1.5 K using continuous laser excitation at 514 nm. Indicated are the fields B_1 and B_2 at which the ENDOR experiments have been performed. The dotted curve shows the simulation of the EPR spectrum.

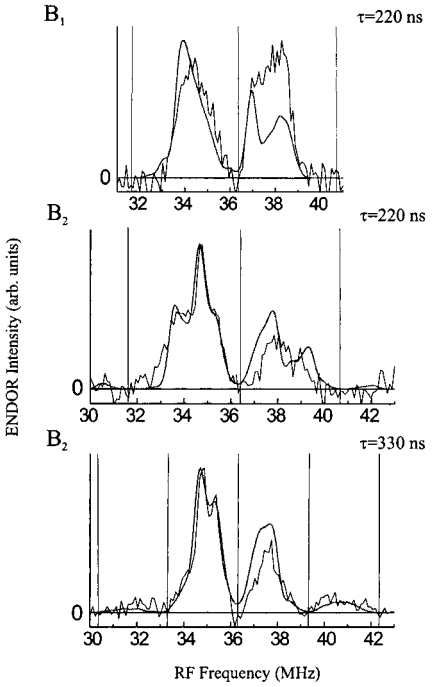

Figure 2. ENDOR spectra of a frozen solution of C_{70} at 1.5 K at the fields B_1 (upper panel) and B_2 (middle and lower panel) and corresponding simulations using the spin densities in Table 1. The two upper spectra were recorded using a value for τ of 220 ns, the lower one using a value for τ of 330 ns. The thin vertical lines indicate the "blind spots" for pulsed ENDOR according to eq 2.

Pulsed ENDOR spectra of a frozen solution of 15% ^{13}C enriched C_{70} at 1.5 K are shown in Figure 2 for the fields B_1 and B_2. For the field B_1, the ENDOR spectrum shows two broad, almost equally intense, bands, one below and one above the ^{13}C nuclear Zeeman frequency ν_z of about 36.3 MHz. For the field B_2 and a value for τ of 220 ns, a relatively narrow band shows up at 34.8 MHz with a broad shoulder toward lower frequency and a less pronounced shoulder toward higher frequency. To the right of ν_z, a broad band is seen that carries less than half the intensity of the band at 34.8 MHz. The spectrum at field B_2 and a value for t of 330 ns shows, besides band shapes that are different from those in the spectrum with a value for τ of 220 ns, intensity up to about 42 MHz.

Data Analysis

The ENDOR spectra of C_{70} have been analyzed in a similar way to those of C_{60} previously.[8] The hyperfine interaction of the triplet electron spin with each of the ^{13}C nuclear spins comprises an isotropic and an anisotropic contribution. The isotropic contribution, determined by the electron-spin density at the nucleus, will be indicated by $a_{iso,i}$, where i (=1−5) refers to the symmetry inequivalent nuclei in the C_{70} molecule. The anisotropic contribution concerns the dipole−dipole interaction of the electron-spin density and the nuclear spins. Two-center contributions are found to be negligible, and one-center contributions have been calculated through modeling of the electron-spin distribution around the nuclei. It is assumed that the only orbital that carries spin density at each atom concerns the radial atomic orbital. On the basis of the observation of a negligibly small s-character of this orbital for C_{60}, this orbital is modeled as a pure p orbital. The anisotropic hyperfine tensor becomes axial and for spin density ρ in this orbital may be written as ρA with $A_{\xi\xi}$=184 and $A_{\eta\eta} = A_{\zeta\zeta} = -92$ MHz.[12] Here ξ, η, and ζ refer to a local orthogonal axis system at the ^{13}C atom with ξ in the radial direction.

The experiments concern a random distribution of C_{70} molecules in a frozen solution. The orientations of the molecules that contribute to the echo intensity at either B_1 or B_2 have been determined through the simulation of the EPR spectrum shown in Figure 1. For each orientation we have calculated the ^{13}C nuclear resonance frequencies ν_+, ν_0, and ν_- in the triplet sublevels T_{+1}, T_0, and T_{-1} according to the nuclear-spin Hamiltonian

$$H_n = -\mu_n g_C \vec{I}\cdot\vec{B} + \langle\vec{S}\rangle\cdot\vec{A}\cdot\vec{I} \qquad (1)$$

for each of the 70 carbon atoms in C_{70}, taking into account the orientation of $\vec{B}$ in the local axes system (ξ, η, ζ). In eq 1, μ_n is the nuclear Bohr magneton and $\langle S\rangle$ is the expectation value of the electron spin angular momentum operator. Additionally, we have to include the ENDOR efficiency function[13]

$$F_{ENDOR} = \frac{1}{2}\sin^2(\pi(\nu_{RF} - \nu_z)\tau) \qquad (2)$$

which effectively removes the intensity at the nuclear Zeeman frequency (ν_z) from the spectrum and introduces so-called "blind spots" at $\pm n/\tau$ (n = 1, 2, ...) MHz from ν_z. In eq 2, ν_{RF} is the frequency of the RF wave and τ is the separation between the first and the second microwave pulse. If a nuclear resonance is represented by a stick, then for each orientation each ^{13}C nucleus contributes two sticks at ν_+ and ν_- to the ENDOR spectrum with amplitudes determined by the contribution of that orientation to the EPR intensity at the corresponding magnetic field and the ENDOR efficiency. The pulsed ENDOR spectrum is obtained by summing over the grid of molecular orientations and dressing the resulting histogram with Gaussian functions.

The lowest triplet state of C_{70} belongs to the A_2' irreducible representation of D_{5h}. In terms of a molecular-orbital description, this state derives from the excitation of an electron from the highest occupied to the lowest unoccupied molecular orbital (HOMO and LUMO), which belong to a_2'' and a_1'', respectively.[14] Because both molecular orbitals are antisymmetric and the p atomic orbitals on the atoms of type 5 are symmetric under reflection in the equatorial plane of the molecule, the atoms of type 5 will have zero coefficients both in the HOMO and in the LUMO; i.e., the spin density on the atoms of type 5 is zero.

At field B_1 (upper panel in Figure 2) there is ENDOR intensity on both sides of the nuclear Zeeman frequency. At this field, molecules are selected that have their fine-structure z-axis parallel to the magnetic field. In combination with the diagonal values of the anisotropic hyperfine tensor and the

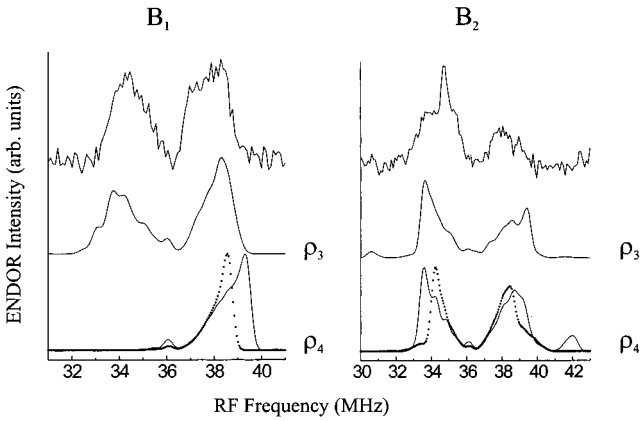

Figure 3. Upper traces show ENDOR spectra recorded at field B_1 (left) and B_2 (right), using a value for τ of 220 ns. The other traces show calculated ENDOR spectra for hypothetical C_{70} molecules that only carry spin density on the atoms of type 3 (middle traces) or type 4 (lower traces). The lower straight traces have been optimized to the low-frequency edge at field B_2, the lower dotted traces to the high-frequency edge at field B_1.

positive sign of D, this implies that atoms of type 4 contribute at the high-frequency side of ν_z ($\vec{B} \perp \xi$), atoms of type 1 and 2 on the low-frequency side ($\vec{B} // \xi$), and atoms of type 3 on both sides. The edge of the spectrum at the high-frequency side corresponds to a frequency shift of 2.3 MHz with respect to ν_z. If this shift derives from atoms of type 4, it would correspond to atoms with their ξ axis about perpendicular to $\vec{B}$, and intensity should therefore also be visible at the low-frequency side at field B_2. The corresponding spectrum in Figure 2 shows on the low-frequency side edges at 3.0, 1.6, and 1.0 MHz from ν_z only. Consequently, the high-frequency edge at field B_1 probably does not derive from atoms that have their ξ axis perpendicular to $\vec{B}$. The only other atoms that can contribute at the high-frequency side of ν_z at field B_1 are those of type 3. To simulate the edge at 2.3 MHz from ν_z, these atoms should carry a spin density of about 3.3%. The middle traces in Figure 3 show calculated ENDOR spectra at the fields B_1 and B_2 and a τ of 220 ns, for a hypothetical C_{70} molecule that only carries 3.3% spin density on the atoms of type 3. Both the high-frequency edge at field B_1 and the low-frequency edge at field B_2 are simulated in accordance with the experiment. The measured ENDOR spectrum at field B_1 shows a steep increase of intensity above ν_z around 36.5 MHz. This behavior is not simulated using only the atoms of type 3, which indicates a strong second transition close to ν_z at its high-frequency side. This can only derive from the atoms of type 4, which then have to carry a spin density of about 1%, which implies that the atoms of type 3 and 4 together account for about 85% of the total spin density.

The best simulations of the ENDOR spectra were obtained with the remaining spin density on the atoms of type 1. The simulations could be further improved when an isotropic hyperfine interaction of -0.3 MHz was introduced on the atoms of type 1 and optimum values of the spin densities are summarized in Table 1. The corresponding simulations are shown in Figure 2. Besides the edges of the ENDOR spectra at field B_1, and the spectrum at field B_2 with a value for τ of 220 ns, also the spectrum at B_2 with a τ of 330 ns is simulated correctly, both as regards the two bands to the left of ν_z and the intensity between 40 and 42 MHz.

Discussion

On the basis of the three ENDOR spectra shown in Figure 2, we have derived the spin-density distribution for the lowest triplet state of C_{70}. According to this analysis, 66% of the triplet electron spin is on the atoms of type 3, 20% on the atoms of type 4 and 16% on the atoms of type 1. The simulations shown in Figure 2 provide a satisfactory description of the experimental data but show some shortcomings. Particularly above the nuclear Zeeman frequency, the experimental line shapes could not completely be reproduced. Below we will first comment on the assumptions underlying the analysis and then elucidate on the interpretation.

TABLE 1: Spin Densities in the Lowest Triplet State of C_{70}, As Derived from ENDOR

atom	abundance	triplet spin density (%)
1	10	1.6 ± 0.2;
2	10	<0.3
3	20	3.3 ± 0.3
4	20	1.0 ± 0.3
5	10	0

To translate the observed ENDOR shifts into electron-spin densities, we assumed that the triplet wave function is built up from pure p orbitals on the individual atoms. In view of the curvature of the surface of the C_{70} molecule, molecular orbitals that include some s-character might seem more appropriate. However, for C_{60} a description in terms of hybridized atomic orbitals, whose s character is determined by the local geometry, was found to largely overestimate the s character.[8] The introduction of a little s character for C_{70} would be arbitrary. We estimate the corresponding error in the anisotropic hyperfine tensor, and consequently in the spin densities, to be less than 3%. Additional simulations of the ENDOR spectra indicated that we cannot exclude isotropic hyperfine contributions $a_{iso,3}$ between -0.3 and 0 MHz and $a_{iso,4}$ between -0.3 and 0.3 MHz. The simulations improved when we added an $a_{iso,1}$ of -0.3 MHz. This isotropic hyperfine interaction for atoms of type 1 looks plausible because the curvature of the C_{70} molecule is largest at the pole.

The fine-structure parameter E of C_{70} is small but not zero. Nevertheless, the molecule has been treated as axially symmetric, i.e., with 5 inequivalent carbon atoms. The nonaxiality means that the spin densities in fact vary among atoms of the "same" type. The quality of the simulations shows that this variation must be small, which agrees with the large ratio D/E of about 7.

The C_{70} molecule pseudorotates around its z-axis at a rate of about 1 μs^{-1} at liquid-helium temperatures. This pseudorotation barely influences the ENDOR spectra. Pseudorotation does not involve a real rotation of the molecule, but merely a collective motion of all atoms over distances of the order of 0.01 Å. Because E differs from zero, the pseudorotation around z may change the EPR frequency of the molecule, but the orientation of the local hyperfine tensors with respect to the external magnetic field will be virtually unaffected.

The sharp line at 34.8 MHz and its two shoulders observed at the low-frequency side of ν_z for field B_2 and $\tau = 220$ ns, provide clear indications for three spin densities. The largest spin density is responsible for the low-field edge at about 33 MHz and cannot be on the atoms of type 4. The lower traces in Figure 3 show simulated ENDOR spectra corresponding to a hypothetical C_{70} molecule with spin density on the atoms of type 4 only. For the set of bold curves the spin density has been optimized to the low-frequency edge at field B_2 (3.3%), for the other to the high-frequency edge at field B_1 (2.5%). Neither of the sets reproduces both edges, and as both edges concern the same component of the hyperfine tensor ($\xi \perp B$), an isotropic hyperfine interaction will not solve this problem.

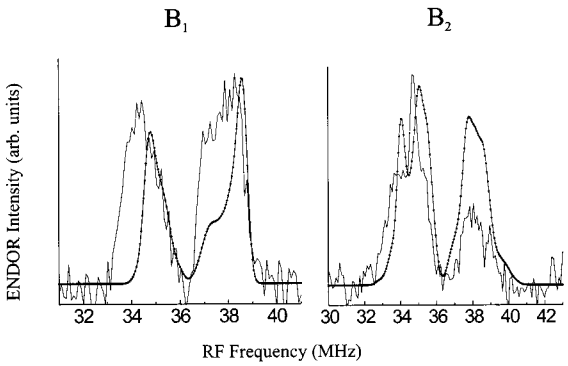

Figure 4. Calculated ENDOR spectra corresponding to a value for τ of 220 ns at the fields B_1 (left) and B_2 (right). In these calculated spectra the spin densities have been used that are calculated quantum chemically. For comparison also the experimental ENDOR spectra are shown.

Only the set corresponding to 2.5% spin density may be acceptable, because it does not introduce intensity in regions where the measured intensity is zero. In that case, to simulate the low-field edge at field B_2 one of the three other atoms would need a spin density of 3.3%. First, this would lead to a total spin density much higher than 100%, second this would introduce features in the spectra that are not observed. The largest spin density of 3.3% has to be on the atoms of type 3.

A second pronounced feature in the spectrum at field B_2 and $\tau = 220$ ns is the intensity of the line at 34.8 MHz. The only way to correctly simulate its large intensity with respect to that of its shoulders, is by assigning this line to atoms of type 1. For this field, molecules are selected with the ξ axes of all atoms of type 1 about perpendicular to $\vec{B}$. They all contribute at approximately the same frequency, while for atoms further away from the poles there is a spread in orientations of the ξ axes and consequently in the hyperfine interactions.

We have compared the experimentally determined spin densities with values calculated quantum chemically. A restricted Hartree−Fock SCF triplet-state calculation has been performed, using the MINDO/3 Hamiltonian in the MOPAC 93 package, followed by configuration interaction. The ground-state geometry of D_{5h} symmetry has been taken from ref 15. In the configuration interaction calculation the 24 singly excited configurations have been considered that can be constructed by promoting an electron from one of the four HOMOs to one of the three LUMOs. In accordance with the analysis of the phosphorescence spectra[7] and with calculations by Surján et al.,[9] the lowest triplet state is found to belong to the A_2' irreducible representation. This lowest triplet state is not a pure configuration, but consists of contributions from three determinants, with weights of 64%, 18%, and 18%. The main contribution corresponds to the promotion of an electron from the a_2'' HOMO to the a_1'' LUMO, the others to the promotion of an electron from one of the doubly occupied to one of the unoccupied e_1'' molecular orbitals. According to the calculations, the atoms of type 4 would carry 2.7% spin density, of type 3 1.6%, of type 2 0.6%, and of type 1 0.9%. These values are in line with the qualitative picture drawn by Surján et al.[9] but differ significantly from the experimentally determined spin densities.

Calculated ENDOR spectra based upon the calculated spin densities are shown in Figure 4. The deviations concern at field B_1 the low-frequency edge and the intensity closely above ν_z, at field B_2 the low-frequency edge, the shape at the low-frequency side, and the intensity ratio between the low- and high-frequency side of the spectrum. For a proper comparison one should calculate the ENDOR spectra on the basis of hyperfine tensors that can be derived from the triplet wave function. The present analysis, however, already indicates that the quality of the calculation is limited. Probably, this is caused by the small size of the configuration interaction (24 determinants). The calculations show that the spin-density distribution corresponding to the $e_1'' \Rightarrow e_1''$ determinant differs significantly from that corresponding to the $a_2'' \Rightarrow a_1''$ determinant, which indicates that a larger CI may lead to a different spin-density distribution. For the lowest excited singlet states of C_{70}, Negri et al. reported drastic changes of the energies when doubly excited configurations are included in the configuration interaction.[16]

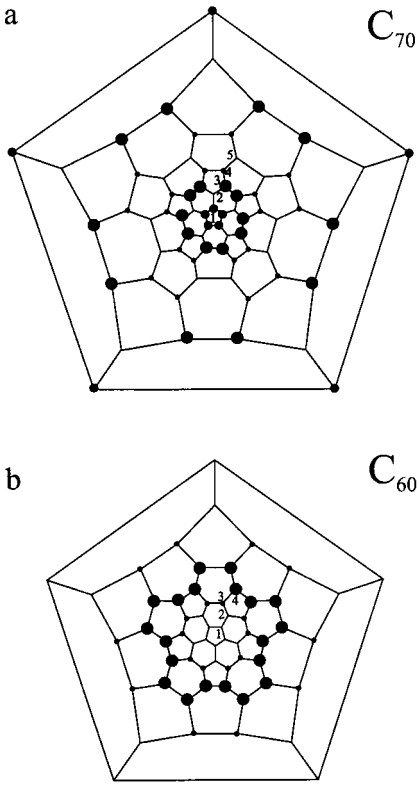

Figure 5. Schlegel diagrams for C_{70} (a) and C_{60} (b), where the dots schematically indicate the experimentally determined electron-spin densities for the triplet states of these molecules. The data for C_{60} have been taken from ref 8.

Finally, we compare our results obtained for the triplet states of C_{70} and C_{60}.[8] Figure 5 shows the Schlegel diagram for both molecules, where the sizes of the dots schematically indicate the spin densities on the different atoms as they result from our analysis of the ENDOR spectra for both molecules. The simplest picture of the C_{70} molecule would be that of a C_{60} molecule with an inserted belt of 10 atoms that do not carry spin density. This picture is not valid, as the spin-density distribution in the triplet state of C_{70} is more polar than for C_{60}. For C_{60} the atoms of type 4 carry 3.8%, the atoms of type 3 1.0%, and the atoms of type 1 and 2 virtually nothing. For C_{70} the atoms of type 4 carry only 1.0%, the atoms of type 3 3.3% and the atoms of type 1 1.6%. The spin-density distribution determines the spin−spin interaction, which in turn determines the fine-structure interaction. Whether the difference in spin-density distribution between C_{60} and C_{70} explains the values of D, −340 MHz for C_{60} and +150 MHz for C_{70}, is the subject of a forthcoming paper.

Acknowledgment. This work is part of the research program of the "Stichting voor Fundamenteel Onderzoek der Materie"

(FOM) and has been made possible by financial support from the "Nederlandse Organisatie voor Wetenschappelijk Onderzoek" (NWO).

References and Notes

(1) Arbogast, J. W.; Darmanyan, A. P.; Foote, C. S.; Rubin, Y.; Diederich, F.; Alvares, M. M.; Anz, S. J.; Whetten, R. L. *J. Phys. Chem.* **1991**, *95*, 11−12.

(2) Arbogast, J. W.; Foote, C. S. *J. Am. Chem. Soc.* **1991**, *113*, 8886−8889.

(3) Wasielewski, M. R.; O'Neil, M. P.; Lykke, K. R.; Pellin, M. J.; Gruen, D. M. *J. Am. Chem. Soc.* **1991**, *113*, 2774−2775.

(4) van den Heuvel, D. J.; Chan, I. Y.; Groenen, E. J. J.; Schmidt, J.; Meijer, G. *Chem. Phys. Lett.* **1994** *231*, 111−118.

(5) Bronsveld, M. V.; Dauw, X. L. R.; Groenen, E. J. J. *Chem. Phys. Lett.* **1998**, *293*, 528−534.

(6) Dauw, X. L. R.; Poluektov, O. G.; Warntjes, J. B. M.; Bronsveld, M. V.; Groenen, E. J. J. *J. Phys. Chem. A* **1998**, *102*, 3078−3082.

(7) Warntjes, J. B. M.; Holleman, I.; Meijer, G.; Groenen, E. J. J. *Chem. Phys. Lett.* **1996**, *261*, 495−501.

(8) Dauw, X. L. R.; van den Berg, G. J. B.; van den Heuvel, D. J.; Poluektov, O. G.; Groenen, E. J. J. *J. Chem. Phys.* **2000**, *112*, 7102−7110.

(9) Surján, P. R.; Németh, K.; Kállay, M. *J. Mol. Struct. (THEOCHEM)* **1997,** *398*, 293−300.

(10) Taylor, R.; Hare, J. P.; Abdul-Sada, A. K.; Kroto, H. W. *J. Chem. Soc., Chem. Commun.* **1990**, 1423−1425.

(11) Disselhorst, J. A. J. M.; van der Meer, H.; Poluektov, O. G.; Schmidt, J. *J. Magn. Reson. A* **1995**, *115*, 183−188.

(12) Groenen, E. J. J.; Buma, W. J.; Schmidt, J. *Isr. J. Chem.* **1988**, *29*, 99−108.

(13) Gemperle, C.; Sørensen, O. W.; Schweiger, A.; Ernst, R. R. *J. Magn. Reson.* **1990,** *87*, 502−515.

(14) Scuseria, G. E. *Chem. Phys. Lett.* **1991**, *180*, 451−455.

(15) van Smaalen, S.; Petricek, V.; de Boer, J. L.; Dusek, M.; Verheijen, M. A.; Meijer, G. *Chem. Phys. Lett.* **1994**, *223*, 323−328.

(16) Negri, F.; Orlandi, G. *J. Chem. Phys.* **1998**, *108*, 9675−9684.